NANO LETTERS

2008
Vol. 8, No. 8
2299-2304

Burning Match Oxidation Process of Silicon Nanowires Screened at the Atomic Scale

Paola De Padova,*,† Christel Leandri,‡ Sebastien Vizzini,‡ Claudio Quaresima,† Paolo Perfetti,† Bruno Olivieri,§ Hamid Oughaddou,|| Bernard Aufray,‡ and Guy Le Lay‡

CNR-ISM, via Fosso del Cavaliere 100, 00133 Roma, Italy, CINaM-CNRS, Campus de Luminy, Case 913, 13288 Marseille Cedex 9, France, CNR-ISAC, via Fosso del Cavaliere 100, 00133 Roma, Italy, and Commissariat à l'Energie Atomique, Laboratoire SIMA, DSM-IRAMIS-SPCSI, Bat. 462, Saclay, Gif sur Yvette cedex, France, and Département de Physique, Université de Cergy-Pontoise, 95031 Pontoise cedex, France

Received April 7, 2008

ABSTRACT

Silicon oxide nanowires hold great promise for functional nanoscale electronics. Here, we investigate the oxidation of straight, massively parallel, metallic Si nanowires. We show that the oxidation process starts at the Si NW terminations and develops like a burning match. While the spectroscopic signatures on the virgin, metallic part, are unaltered we identify four new oxidation states on the oxidized part, which show a gap opening, thus revealing the formation of a transverse internal nanojunction.

Si NWs could be the building blocks of many functional nanoscale electronic devices. In this respect, a number of Si NWs−based transistors have been already demonstrated[1–4] and a strong endeavor to exploit such nanowire structures is pursued.[5,6] Elevated synthesis temperature has been used to generate defect free SiO_2 saturated crystalline silicon nanowires through a mixture of $Si-SiO_2$.[7,8] Furthermore, straight, aligned silica nanowires with an helical SiO_x internal structure have been produced through a Co−catalyzed process.[9]

For decades, the oxidation of silicon has been an issue of paramount importance in many areas of physics and technology since the interface between silicon and silicon dioxide plays a crucial role in microelectronics devices.[10–23] With their continuous down-sizing to the nanoscale, the role played by this interface becomes prevalent.[24] From the theoretical point of view, recent ab initio calculations[24] have been used to study the influence of doping on the conductance of surface-passivated Si NWs. Clearly, the role of the surface dangling bond defects becomes of crucial importance when the surface to bulk ratio in the NWs increases as a result of their size reduction.

In spite of the numerous studies on the $Si-SiO_2$ interface[10–24] it is still very difficult to give a consistent description of the nanoscopic bond arrangement at this interface, mainly because of the fact that the interface is buried and has only short-range order. Numerous experimental techniques including X-ray scattering,[10] photoelectron spectroscopy,[11] and scanning probe microscopy,[12] as well as theoretical calculations[13–17] have been used to model the still controversial microscopic structure of the thermally grown Si(001)− and $Si(111)-SiO_2$ interfaces.[11–23] Up to now, core-level PES[11,18–23] has been the most successful tool for the investigation of the $Si-SiO_2$ interfaces; indeed, the Si 2p CL from clean or oxidized silicon surfaces is undoubtedly the most widely scrutinized spectral feature in PES. It is well-known that the Si 2p spectrum of this interface comprises five distinct peaks; three of them are assigned to interfacial silicon atoms[11–23] while the other two are assigned to bulk silicon and bulk SiO_2. So, there is a large consensus to attribute the various suboxide peaks to Si atoms with a different number of nearest-neighbor O atoms: one, two, three, or four and to refer to formal oxidation states as Si^{1+}, Si^{2+}, Si^{3+} and Si^{4+}. This empirical assumption, based on a charge-transfer model, is generally accepted and gives the

* Corresponding author. E-mail: paola.depadova@ism.cnr.it. Phone:+39-06-49934144. Fax:+39-06-49934153.
† CNR-ISM.
‡ CINaM-CNRS.
§ CNR-ISAC.
|| Commissariat à l'Energie Atomique, Laboratoire SIMA, DSM-IRAMIS-SPCSI.

10.1021/nl800994s CCC: $40.75
Published on Web 07/12/2008

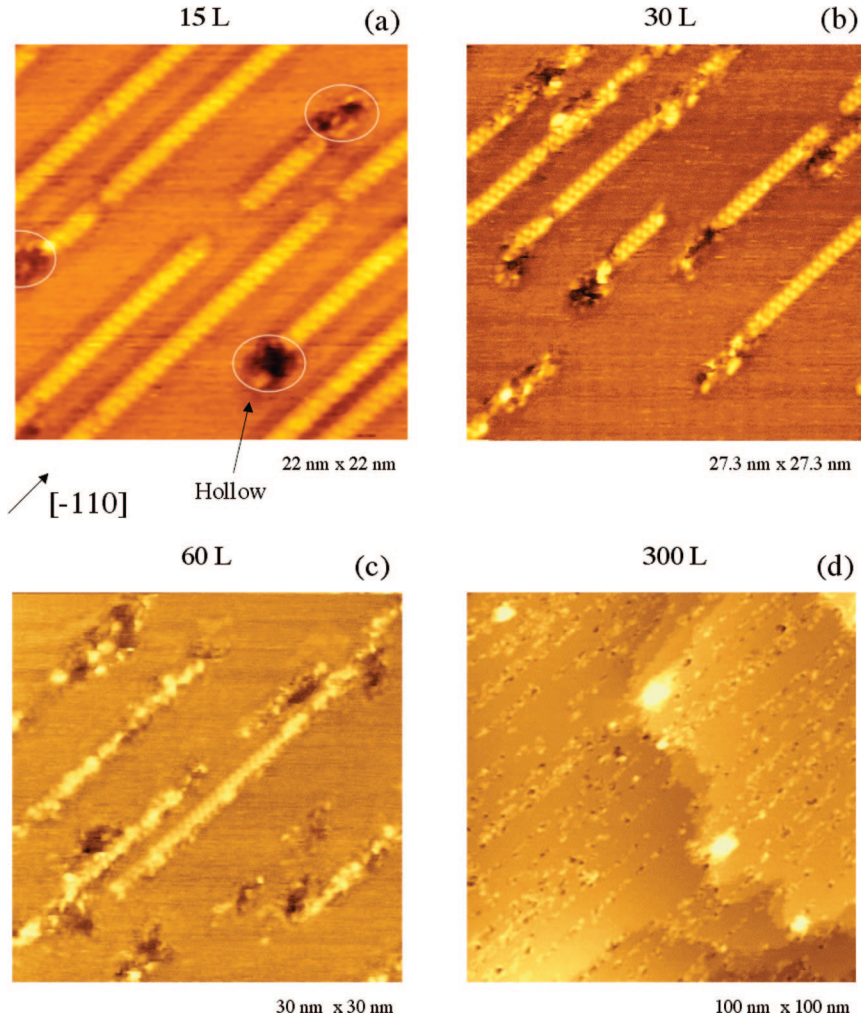

Figure 1. Filled-states STM images of Si NWs on Ag(110) at different oxygen doses. (a) 22 × 22 nm^2 at 15 *L*. (b) 27.3 × 27.3 nm^2 at 30 *L*. (c) 30 × 30 nm^2 at 60 *L*. (d) 100 × 100 nm^2 at 300 *L*.

four well-separated chemically shifted components on the Si 2p PES spectrum.

Diverse interpretations suggest a chemically graded interface with all Si^{1+}, Si^{2+}, Si^{3+} suboxides and Si^{4+} silica distributed over a thickness ranging from about 0.2 to 3.0 nm.[11,14,18] Others propose a silicon−silica interface consisting of a single layer of silicon atoms in a +2 oxidation state,[16,17,20] with Si^{3+} and Si^{1+} fragments only present at steps.[25] Comparatively, in the case of the Si(111)−SiO_2 interface, the proposed model[21] is based on the concept of statistical cross-linking between the dangling bonds from the two sides of the interface plane. Finally, by transmission electron microscopy, it was observed that the transformation of crystalline Si to amorphous SiO_2 occurs via an ordered crystalline oxide layer of trydimite, the stable bulk form of SiO_2, with a typical thickness of about 0.5 nm.[26]

This communication reports a unique combined study of the oxidation process at the atomic scale on a prototypical, well-characterized system, namely, a massively parallel array of Si NWs, just 1.6 nm in width and about 0.2 nm in height[27,28] by scanning tunneling microscopy/spectroscopy (STM/STS) and high-resolution (HR) Si 2p core-level photoelectron spectroscopy (PES). At the early stages of oxygen adsorption, the oxidation process takes place only at the Si NW terminations; at increasing doses, this process develops like a burning match along the [−110] direction, keeping the one-dimensional orientation of the NWs.

In excellent agreement with STM measurements, the HR photoemission spectroscopy shows the presence of all components related to the virgin SiNWs, Si^0, in addition to the oxidation components, Si^{1+}, Si^{2+}, Si^{3+}, and Si^{4+} on the features of the Si 2p core−levels. STS measurements indicate a metallic behavior on the virgin part of the SiNWs and a gap opening of ∼0.35 V on the oxidized part, revealing the formation of an internal nanojunction.

The HR−PES experiments were carried out at the VUV beam line of the Italian synchrotron radiation facility ELETTRA in Trieste, whereas the STM and STS observations of the SiNWs were performed at the CINaM in Marseille. In both laboratories the same procedure has been used for sample preparation, silicon evaporation and Si oxidation. The Ag(110) substrate was cleaned in the UHV chamber (base pressure: 8.5 × 10^{-11} mbar) by repeatedly sputtering with Ar^+ ions and annealing the substrate at 750 K, while keeping the pressure below 2 × 10^{-10} mbar during the heating. Silicon was evaporated at a rate of ∼0.03 ML/

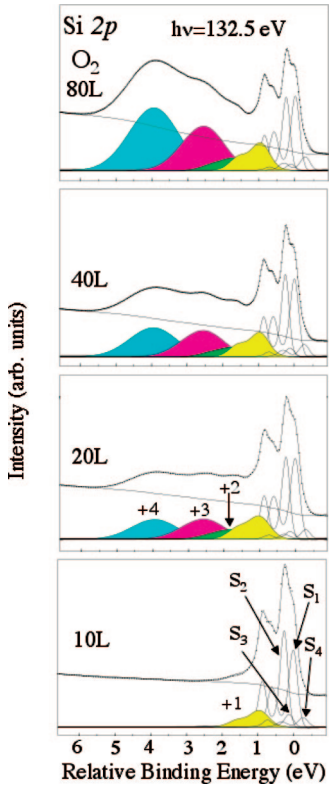

Figure 2. Convoluted Si 2p core levels. Oxygen exposure of SiNWs grown on Ag(110) at 10 *L*, 20 *L*, 40 *L*, and 80 *L*. The colored components (S^{1+}, S^{2+}, S^{3+}, and S^{4+}) related to the different oxidation states (+1 to +4) grow at the expense of the four initial components (S_1, S_2, S_3, S_4) of the clean SiNWs.

min from a silicon source in order to form the Si NWs[27,28] while the Ag substrate was kept at room temperature (RT). The oxidation was obtained upon exposing the so-formed Si NWs at several increasing total doses expressed in Langmuir (1 $L = 1 \times 10^{-6}$ Torr per 1s) 10, 20, 40, 80, and 300 *L* of pure molecular oxygen (99.999%) also at RT.

The photoemission spectra were acquired using an electron energy analyzer with an acceptance of 8°, set at an emission angle of $\vartheta = 45°$. The angle between the photon beam and the normal to sample surface was also 45°. The photon energy was 132.5 eV, while the total energy resolution was better than 50 meV. All STM images presented were recorded at RT in constant-current mode at a bias voltage of −1.8 V and a tunneling current of 1.2 nA.

Figure 1a displays a 22 × 22 nm^2 filled-states STM image of ∼0.5 ML Si deposited at RT on the Ag(110) surface exposed to a 15 *L* dose of oxygen. This high resolution STM image shows the massively parallel Si NWs, all aligned along the [−110] direction of the Ag(110) surface with a *x*2 periodicity, that is, $2a_{Ag[-110]}$. We directly see the termination sides of the clean Si NWs drastically modified, showing apparently some black voids or hollows (circled images in Figure 1a) that announce the onset of the oxidation process. These termination sides are involved at first in the oxidation process, whereas the almost totality of the Si NWs is not affected by the O_2 atoms.

At higher oxygen exposure, the oxidation of the Si NWs proceeds progressively from their extremities along the [−110] direction maintaining an atomic structure preferably developed along the one-dimension of the wires. This is clearly observed in the Figure 1b,c, which display respectively 27.3 × 27.3 nm^2 and 30 × 30 nm^2 filled-states STM images at 30 *L* and 60 *L* of oxygen exposure. The oxidation behaves according to a match-burst process, where the

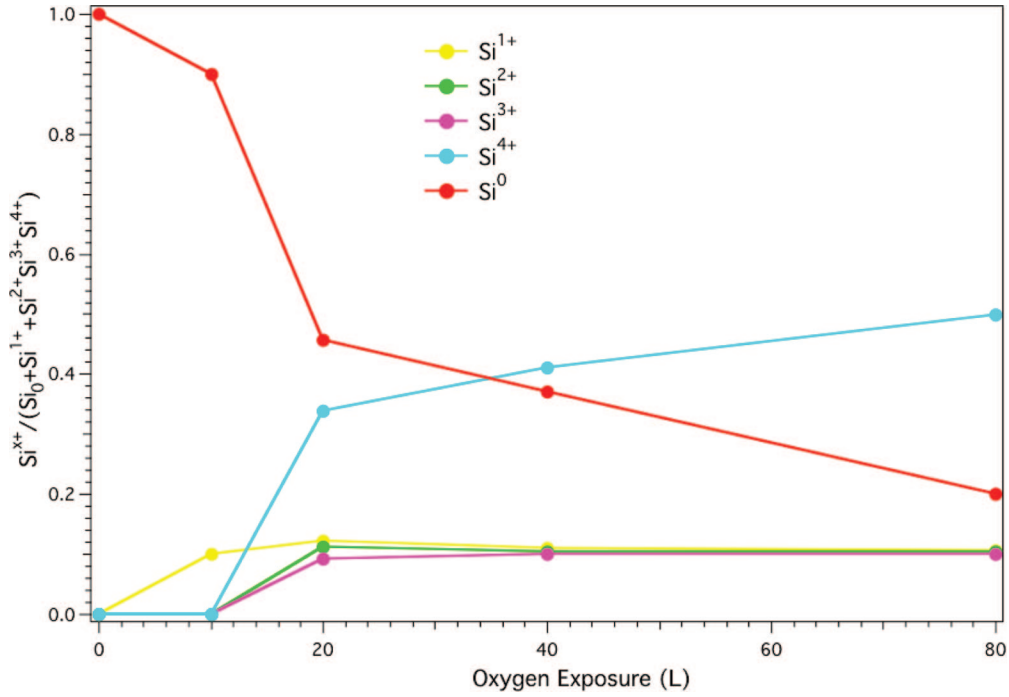

Figure 3. Fractional intensities of the convoluted Si 2p components. S^0, S^{1+}, S^{2+}, S^{3+}, and S^{4+} relative intensities, measured at 132.5 eV photon energy, are plotted versus the oxygen exposure of the clean Si NWs. S^0 is the intensity sum of the S_1, S_2, S_3, and S_4 components.

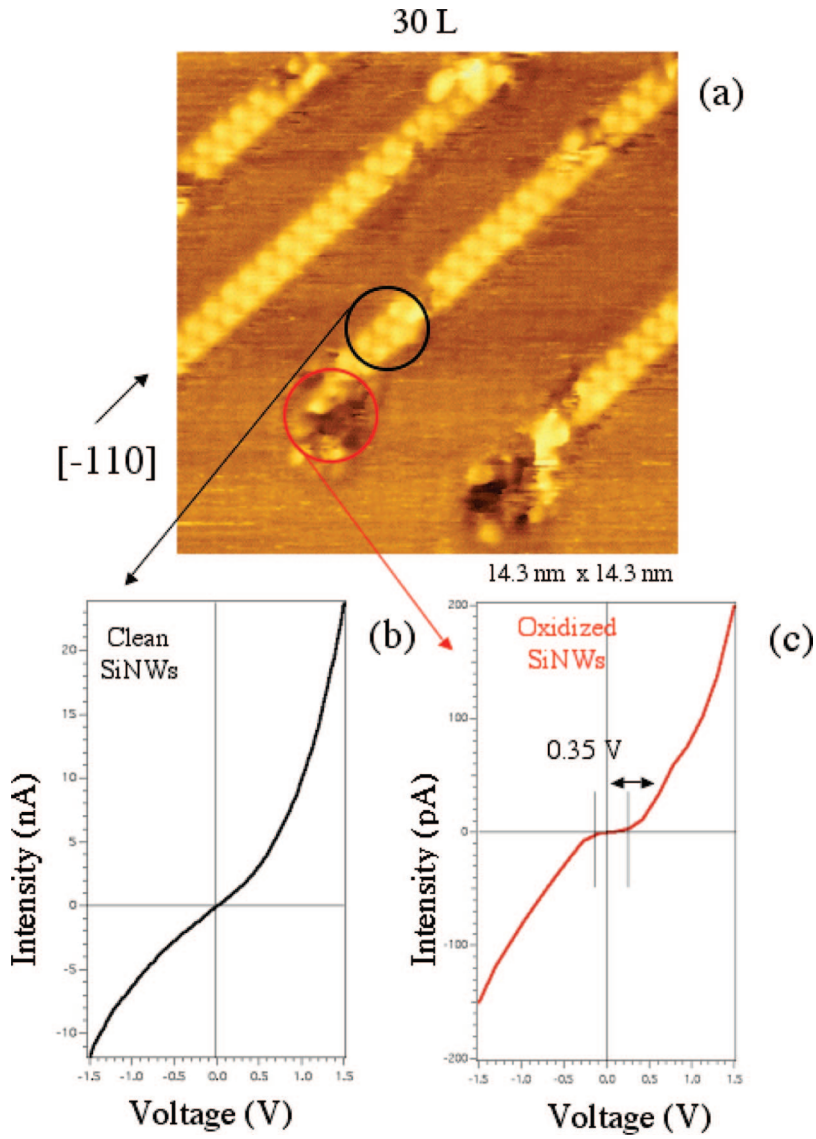

Figure 4. Scanning tunneling microscopy of Si NWs exposed to 30 *L* O_2 and *I*−*V* curves. (a) 14.3 × 14.3 nm^2 filled-states image. (b) *I*−*V* on clean Si NWs. Selected areas on the STM image indicate where the *I*(*V*) curves are collected. (c) *I*−*V* characteristics of oxidized Si NWs.

extremities of the Si NWs are considered as the head of a match, which reacts with the oxygen atoms. This behavior implies that the termination sides of the Si NWs comprise several extremely reactive dangling bonds, able to be rapidly saturated by the oxygen atoms. In this way, the oxidation propagates along the [−110] direction, like a flame front, which is the interface, which separates the clean and the oxidized parts of the Si NWS. Subsequently, at 300 *L* of O_2 exposure, we observe in Figure 1d, which shows a large 100 × 100 nm^2 filled-states STM image, the massively oxidized Si nanostructures on different terraces of the Ag(110) surface.

These characteristic features discovered through the HR STM observations of the oxidized Si NWs find their corresponding signatures in spectroscopy measurements. Figure 2 reports the Si 2p core-level spectra measured on the Si NWs, after 10, 20, 40, and 80 *L* of O_2 exposure. Noticeably, the figure shows that the Si peak is strongly modified during the O_2 exposure at increasing doses. The clean Si NWs on Ag(110) have been recently characterized by HR core-level photoemission spectroscopy[28] by convoluting the spectra with spin−orbit (S−O) split, asymmetric Doniach−Sunijch functions. A least-squares fitting procedure after a Shirley background subtraction revealed four doublets, S_1, S_2, S_3, S_4, each with a S−O splitting of 609 ± 5 meV, a branching ratio (BR) of 0.53 and, especially, an asymmetry parameter of 0.122, which indicated that the Si NWs exhibit a strong metallic character.

After oxidation, further quantitative information is obtained by convoluting the Si spectra at their higher binding energy (BE) regions with new additional spin−orbit split symmetric Voigt function doublets (still, S−O splitting = 609 meV and BR = 0.53). Here, the BE is considered relative to the position of the S_1 core level of the clean silicon NWs (set at 0 eV).

Thus, we identify on the Si 2p PES spectra of the Si NWs at higher BE four new peaks S^{1+}, S^{2+}, S^{3+}, and S^{4+} located at +0.95, +1.71, +2.42, and +3.85 eV. We assign them to

the +1, +2, +3 and +4 oxidation states of Si, in perfect agreement with the chemically shifted components found at the Si(001)− and Si(111)−SiO_2 interfaces.[11] For these chemically shifted components, we found full widths at half-maximum (fwhm) of 0.65, 0.9, 1.15, and 1.26 eV in good agreement with the previous measurements by Himpsel[11] and Lu,[19] the core-hole lifetime, the dynamical phonon broadening, and the static disorder being the main ingredients that contribute to the fwhm enlargements. A point to notice is that each of the Si 2p components of the clean Si NWs as well as their relative weights is preserved.[28]

The behavior of the S^{1+}, S^{2+}, S^{3+}, and S^{4+} relative intensities with increased O_2 exposure is shown in Figure 3 for the Si 2p spectra. Note that the measured intensity of S^{3+} has been corrected by a factor of 1.7, since it has been shown that the intensity is enhanced at the photon energy of 132.5 eV used, mainly due to a cross-sectional resonance.[11]

The figure shows that at the early oxidation stages (10 *L*) only the S^{1+} state takes place; next from 20 *L* O_2 exposure all the Si oxidation states are present but the intensities of S^{1+}, S^{2+}, S^{3+} stay constant. The S^0 intensity (sum of $S_1 + S_2 + S_3 + S_4$) decreases monotonically as a function of increasing O_2 doses, while the S^{4+} oxidation state continues to grow. In view of this behavior, it is reasonable to presume that silica develops like a wake behind the suboxides present at the oxidation front, which propagates along the wires. This unexpected oxidation process resembles a fuse burning on the ground; in other words, it spreads like wildfire. The decline of the S^0 contribution together with the increase of the S^{4+} one is in perfect agreement with the evolution of the STM images as a function of the oxygen exposure (see Figure 1d).

We stress one fundamental point: Si 2p components of the virgin portion of the Si NWs rest unaffected upon the O_2 exposure. Recently, He[29] investigated in a theoretical study the adsorption of Si on the Ag(110) surface with the intent of elucidating the atomic structure of the SiNWs. The author found various adsorption geometries for Si coverage up to two monolayers (MLs). Whereas Si−Ag bonds are stronger than Si−Si bonds at low Si coverages, at higher Si coverages, the formation of Si dimers becomes instead more favorable yielding stable Si NWs on the Ag(110) surface at a coverage of 1.2 ML, in the derived ground-state structure. This ground-state structure presents strong similarity to that of the clean Si(001)-2 × 1 reconstructed surface.[30] Two Si layers would be involved in the formation of these Si NWs: the top Si layer is formed by Si dimers; the second layer below is constituted of Si atoms in contact with the first and the second Ag layers beneath. On the basis of this atomic model for the bare Si NWs, we could have anticipated a vertical growth of the oxides; clearly the horizontal formation of such one-dimensional silica appears to be remarkably original.

Figure 4a shows a 15.8 × 15.8 nm^2 filled-state high-resolution zoom STM image at 30 *L* of O_2, while Figure 4b,c displays corresponding *I*(*V*) spectra measured respectively on both clean and oxidized parts of the Si NWs. On the virgin part, the metallic character is demonstrated by the *I*(*V*) spectra with high currents in the nanoampere regime (Figure 3c). On the contrary, the *I*(*V*) curve acquired on the oxide parts shows a semiconducting behavior revealing a gap of 0.35 V and smaller tunneling currents in the picoampere regime. Hence, it is worth noting that the intensity of the current signal collected on the Si NWS is a factor 10^2 higher than that collected on the oxidized parts, which explains that these parts appear in STM imaging as black voids.

We further stress that the behavior of the curve in Figure 4c can be related to the formation of a junction between the clean and the oxidized Si NWs parts, along the [−110] direction (i.e., along the nanowires). However, we can not exclude a vertical current coming from the tunneling between the oxidized Si NWs and the Ag substrate (along the [110] direction) since a thick SiO_2 film is an insulator (SiO_2 gap ∼ 9 eV), whereas in this case, we have just a small gap of 0.35 V.

In conclusion, during the oxidation of the Si NWs, a very peculiar process takes place along the lengths of the wires, similar to a propagating flame front. All oxidation states (+1, +2, +3, and +4) are present, which is reflected by four oxidation components, S^{1+}, S^{2+}, S^{3+}, and S^{4+} on the Si 2p core level spectra in addition to those related to the still virgin part of the Si NWs. However, the lower oxidation states are confined in the close vicinity of the Si−SiO_2 NWs interface. In perfect agreement with the spectroscopy results, the STM observations reveal the simultaneous coexistence of clean and oxidized parts of the Si NWs. Initially, the oxidation sites are localized at the extremities of the Si NWs. Subsequently, at increasing O_2 doses, they move along the [−110] direction: the oxidation process develops like a burning match. Tunneling spectroscopy measurements confirm the transition from a metallic behavior of the virgin Si NWs to a semiconducting one upon oxidation, with just a narrow gap because of the extreme thinness. The formation of such a transverse internal junction opens up interesting perspectives for future functional nanowire devices at the nanoscale, once the issue of the short-circuiting metallic underlying substrate will be solved; in this respect, work is in progress to encapsulate and extract the massively parallel Si NWs from their silver template.

Acknowledgment. The authors thank the staff of ELETTRA and of the VUV beam line.

Note Added after ASAP Publication: There were errors in the author affiliation in the version published ASAP July 12, 2008; the corrected version was published ASAP July 29, 2008.

References

(1) Friedman, R. S.; McAlpine, M. C.; Ricketts, D. S.; Ham, D.; Lieber, C. M. *Nature* **2005**, *434*, 1085–1085.
(2) Cui, Y.; Lieber, C. M. *Sience* **2001**, *291* (5505), 851–853.
(3) Cui, Y.; Zhong, Z.; Wang, D.; W, U.; Lieber, C. M. *Nano Lett.* **2003**, *3* (2), 149–152.
(4) Wang, D.; Sheriff, B.; Heath, J. R. *Nano Lett.* **2006**, *6* (6), 1096–1100.
(5) Wu, Y.; Cui, Y.; Huynh, L.; Barrelet, C. J.; Bell, D. C.; Lieber, C. M. *Nano Lett.* **2004**, *4* (3), 433–436.

(6) Cui, Y.; Lincoln, J.; Lauhon; M. S.; Mark, S.; Jianfrang, W.; Lieber, C. M. *Appl. Phys. Lett.* **2001**, *78* (15), 2214–2216.
(7) Gole, J. L.; Stout, J. D.; Rauch, W. L.; Wang, Z. L. *Appl. Phys. Lett.* **2000**, *76* (17), 2346–2348.
(8) Lee, S. T.; Wang, N.; Zhang, Y. F.; Tang, Y. H. *MRS Bull.* **1999**, *24* (8), 36–42.
(9) Kim, H. W.; Shim, S. H. *Appl. Surf. Sci.* **2007**, *253* (7), 3664–3668.
(10) Robinson, I. K.; Waskiewicz, W. K.; Tung, R. T.; Bohr, J. *Phys. Rev. Lett.* **1986**, *57* (21), 2714–2717.
(11) Himpsel, F. J.; McFeely, F. R.; Taleb−Ibrahimi, A.; Yarmof, J. A.; Hollinger, G. *Phys. Rev. B* **1988**, *38* (9), 6084–6096.
(12) Ross, F. M.; Gibson, J. M. *Phys. Rev. Lett.* **1992**, *68* (11), 1782–1785.
(13) Ohdomari, I.; Akatsu, H.; Yamakoski, Y.; Kishimoto, K. *J. Appl. Phys.* **1987**, *62* (9), 3751–3754.
(14) Ng, K.-On.; Vanderbilt, D. *Phys. Rev. B* **1999**, *59* (15), 10132–10137.
(15) Pasquarello, A.; Hybertsen, M. S.; Car, R. *Phys. Rev. B* **1996**, *53* (16), 10942–10950.
(16) Buczko, R.; Pennycook, S. J.; Pantelides, S. T. *Phys. Rev. Lett.* **2000**, *84* (5), 943–946.
(17) Tu, Y.; Tersoff, J. *Phys. Rev. Lett.* **2000**, *84* (19), 4393–4396.
(18) Grunthaner, P. J.; Hecht, M. H.; Grunthaner, F. J. *J. Appl. Pyhs.* **1987**, *61* (2), 629–638.
(19) Lu, Z. H.; Graham, M. J.; Jang, D. T.; Tan, K. H. *Appl. Phys. Lett.* **1993**, *63* (21), 2941–2943.
(20) Banaszak Holl, M. M.; Lee, S.; McFeely, F. R. *Appl. Phys. Lett.* **1994**, *65* (9), 1097–1099.
(21) Luh, D.-A.; Miller, T.; Chiang, T.-C. *Phys. Rev. Lett.* **1997**, *79* (16), 3014–3017.
(22) Dreiner, S.; Schürmann, M.; Westphal, C.; Zacharias, H. *Phys. Rev. Lett.* **2001**, *86* (18), 4068–4071.
(23) Dreiner, S.; Schürmann, M.; Westphal, C. *Phys. Rev. Lett.* **2004**, *93* (12), 126101−1126101−4.
(24) Fernandez-Serra, M.-V.; Adessi, Ch.; Blase, X. *Nano Lett.* **2006**, *6* (12), 2674–2678.
(25) Grunthaner, F. J.; Grunthaner, P. J. *Mater. Sci. Rep.* **1986**, *1* (2), 65–160.
(26) Ourmazd, A.; Taylor, D. W.; Rentschler, J. A. *Phys. Rev. Lett.* **1987**, *59* (2), 213–216.
(27) Leandri, C.; Le Lay, G.; Aufray, B.; Girardeaux, C.; Avila, C. J.; Davila, M. E.; Asensio, M. C.; Ottaviani, C.; Cricenti, A. *Surf. Sci. Lett.* **2005**, *574* (1), L9−L15.
(28) De Padova, P.; Quaresima, C.; Perfetti, P.; Olivieri, B.; Leandri, C.; Aufray, B.; Vizzini, S.; Le Lay, G. *Nano Lett.* **2008**, *8* (1), 271–275.
(29) He, Guo-min. *Phys. Rev. B* **2006**, *73* (3), 035311−103511−8.
(30) De Padova, P.; Larciprete, R.; Quaresima, C.; Ottaviani, C.; Ressel, B.; Perfetti, P. *Phys. Rev. Lett.* **1998**, *81* (11), 2320–2323.

NL800994S